Inorg. Chem. **1999,** *38,* 253−259

Dinuclear Phosphido-Bridged Derivatives of Platinum(I). Synthesis and Characterization of $[Pt_2(\mu\text{-}PBu^t_2)_2(PBu^t_2H)(L)]$ [L = PBu^t_2R (R = H, Li, *n*-Heptyl), CO, $\eta^2\text{-}CS_2$]

Piero Leoni,*[†,‡] Giuseppina Chiaradonna,[†] Marco Pasquali,*[†] and Fabio Marchetti[†]

Dipartimento di Chimica e Chimica Industriale, Università di Pisa, I-56126 Pisa, Italy, and
Scuola Normale Superiore, Piazza dei Cavalieri, I-56126 Pisa, Italy

Received September 22, 1998

Contrarily to its palladium analogue, the platinum(II) dihydride $[Pt(\mu\text{-}PBu^t_2)(H)(PBu^t_2H)]_2$ (**3**) does not reductively eliminate molecular hydrogen to the corresponding Pt(I) dinuclear derivative. The transformation can, however, be achieved in a two-step procedure, i.e., by oxidant-induced hydride abstraction from **3**, which produces the cationic monohydride $[Pt_2(\mu\text{-}PBu^t_2)_2(H)(PBu^t_2H)_2]PF_6$, (**4**)$PF_6$, and deprotonation of the latter with a strong base, which produces the desired $[Pt(\mu\text{-}PBu^t_2)(PBu^t_2H)]_2$ (**5**). Complex **5** can be used as the precursor of other neutral bis-phosphido bridged platinum(I) derivatives. For example, carbon monoxide substitutes in mild conditions one of the terminally bonded secondary phosphines and yields quantitatively the monocarbonyl $[Pt_2(\mu\text{-}PBu^t_2)_2(PBu^t_2H)(CO)]$, (**6**), whose crystal and molecular structure was determined by X-ray diffraction. Crystal data: monoclinic, space group $P2_1/n$ (No. 14), $Z = 4$, $a = 9.0910(12)$ Å, $b = 30.527(4)$ Å, $c = 11.903(2)$ Å, $\beta = 93.78(2)°$, $R(F_o) = 0.0378$, $Rw(F_o^2) = 0.0826$ $[I > 2\sigma(I)]$. Complex **6** reacts cleanly with carbon disulfide to give the product of CO substitution $[Pt_2(\mu\text{-}PBu^t_2)_2(PBu^t_2H)(\eta^2\text{-}CS_2)]$ (**9**). Further modifications of complex **5** can be achieved by deprotonating with *n*-BuLi/TMEN one of its secondary phosphines, which produces the lithiated derivative $[Pt_2(\mu\text{-}PBu^t_2)_2(PBu^t_2H)(PBu^t_2Li)]$ (**10**). The latter has been alkylated with 1-bromoheptane to the soluble derivative $[Pt_2(\mu\text{-}PBu^t_2)_2(PBu^t_2H)(PBu^t_2R)]$ (**12**) (R = *n*-heptyl).

Introduction

Platinum chemistry of the oxidation state +1 is much less developed than that of even-numbered oxidation states. It deals mainly with ligand-bridged dinuclear systems, relevant exceptions being the unsupported isonitrile derivatives $[Pt_2(CNR)_4(X)_2]^{z+}$ (X = Cl, $z = 0$;[1] X = CNR,[1,2] PPh$_3$,[3] $z = 2$) and $[Pt_2(CNR)_2(R')_2(PPh_3)_2]$,[4] the cyclopentadienyl $[(\eta^5\text{-}C_5R_5)Pt(CO)]_2$,[5] and $[Pt_2(CO)_2Cl_4]^{2-}$ [6a,b] prepared first in the 1970s with its derivatives $[Pt(CO)Cl(PPh_3)]_2$ [6c] and $[Pt_2(CO)_2(Ar)_2(PPh_3)_2]$.[4] Bis(diphenylphosphino)methane (dppm)-bridged[7] or related complexes[8] constitute the most deeply investigated class of platinum(I) dinuclear derivatives. In other complexes, CO[5b,9] or one of a heterogeneous inventory of ligands[10] reinforces the bond between the metal centers.

We have been involved in recent years in the investigation of palladium(I) di- or trinuclear complexes with bridging phosphido ligands.[11] The precursor of this class of derivatives was $[Pd(\mu\text{-}PBu^t_2)(PBu^t_2H)]_2$ (**1**),[12] which was prepared by the reaction of $CpPd(\eta^3\text{-}C_3H_5)$ with PBu^t_2H and is formed through the elusive Pd(II) intermediate $[Pd(\mu\text{-}PBu^t_2)(H)(PBu^t_2H)]_2$ (**2**) (Chart 1). The platinum analogue of complex **2**, $[Pt(\mu\text{-}PBu^t_2)(H)(PBu^t_2H)]_2$, (**3**),[13] was instead found to be a stable compound which does not eliminate molecular-hydrogen even under

---

[†] Università di Pisa.

[‡] Scuola Normale Superiore.

(1) Yamamoto, Y.; Takahashi, K.; Matsuda, K.; Yamazaki, H. *J. Chem. Soc., Dalton Trans.* **1987**, 1833.

(2) Yamamoto, Y.; Takahashi, K.; Yamazaki, H. *J. Am. Chem. Soc.* **1986**, *108*, 2458

(3) Briant, C. E.; Gilmour, D. I.; Mingos, D. M. P *J. Organomet. Chem.* **1986**, *308*, 381.

(4) Uson, R.; Fornies, J.; Espinet, P.; Fortuño, C.; Tomás, M.; Welch, A. J. *J. Chem. Soc., Dalton Trans.* **1989**, 1583

(5) (a) Boag, N. M.; Goodfellow, R. J.; Green, M.; Hessner, B.; Howard, J. A. K.; Stone, F. G. A. *J. Chem. Soc., Dalton Trans.* **1983**, 2585. (b) Boag, N. M. *Organometallics* **1988**, *7*, 1446.

(6) (a) Boag, N. M.; Goggin, P. L.; Goodfellow, R. J.; Herbert, I. R. *J. Chem. Soc., Dalton Trans.* **1983**, 1101. (b) Goggin, P. L.; Goodfellow, R. J. *J. Chem. Soc., Dalton Trans.* **1973**, 2355. (c) Modinos, A.; Woodward, P. *J. Chem. Soc., Dalton Trans.* **1975**, 1516.

(7) (a) Anderson, G. K. *Adv. Organomet. Chem.* **1993**, *35*, 1. (b) Puddephatt, R. J.; Manojlovic-Muir, L.; Muir, K. W. *Polyhedron*, **1990**, *9*, 2767. (c) Chaudret, B.; Delavaux, B.; Poilblanc, R. *Coord. Chem. Rev.* **1988**, *86*, 191. (d) Brown, M. P.; Puddephatt, R. J.; Rashidi, M.; Seddon, K. R. *J. Chem. Soc., Dalton Trans.* **1977**, 951. (e) Brown, M. P.; Franklin, S. J.; Puddephatt, R. J.; Thomson, M. A.; Seddon, K. R. *J. Organomet. Chem.* **1979**, *178*, 281.

(8) (a) Balch, A. L.; Guimeras, R. R.; Linehan, J.; Wood, F. E. *Inorg. Chem.* **1985**, *24*, 2021. (b) Farr, J. P.; Wood, F. E.; Balch, A. L. *Inorg. Chem.* **1983**, *22*, 3387. (c) Anderson, G. K.; Kuman, R. *J. Organomet. Chem.* **1988**, *342*, 263.

(9) (a) Bandini, A. L.; Banditelli, G.; Cinellu, M. A.; Sanna, G.; Minghetti, G.; Demartin, F.; Manassero, M. *Inorg. Chem.* **1989**, *28*, 404. (b) Knobler, C. B.; Kaesz, H. D.; Minghetti, G.; Bandini, A. L.; Banditelli, G.; Bonati, F. *Inorg. Chem.* **1983**, *22*, 2324. (c) Goodfellow, R. J.; Herbert, I. R.; Orpen, A. G. *J. Chem. Soc., Chem. Commun.* **1983**, 1386. (d) Dixon, A. J.; Firth, S.; Haynes, A.; Poliakoff, M.; Turner, J. J.; Boag, N. M. *J. Chem. Soc., Dalton Trans.* **1988**, 1501.

(10) μ-PR$_2$: (a) Taylor, N. J.; Chieh, P. C.; Carty, A. J. *J. Chem Soc., Chem. Commun.*, **1975**, 448. (b) Siedle, A. R.; Newmark, R. A.; Gleason, W. B. *J. Am. Chem. Soc.* **1986**, *108*, 767. (c) Jans, J.; Naegeli, R.; Venanzi, L. M.; Albinati, A. A.; *J. Organomet. Chem.* **1983**, *247*, C37. (d) Brandon, J. B.; Dixon, K. R. *Can. J. Chem.* **1981**, *59*, 1188. (e) Chatt, J.; Davidson, J. M. *J. Chem. Soc. (A)* **1964**, 2433. (f) Ebsworth, E. A. V.; Ferrier, H. M.; Henner, B. J. L.; Rankin, D. W. H.; Reed, F. J. S.; Robertson, H. E.; Whitelock, J. D. *Angew. Chem., Int. Ed. Engl.* **1977**, *16*, 482. (g) Hadj-Bagheri, N.; Browning, J.; Dehghan, K.; Dixon, K. R.; Meanwell, N. J.; Vefghi, R. *J. Organomet. Chem.* **1990**, *396*, C47. μ-Alkyne: (h) Koie, Y.; Shinuda, S.; Saito, Y.; Fizgerald, B. J.; Pierpont, C. G. *Inorg. Chem.* **1980**, *19*, 770. (i) Koie, Y.; Shinuda, S.; Saito, Y. *Inorg. Chem.* **1981**, *20*, 4408. μ-S: (l) Gaffney, T. R.; Ibers, J. A. *Inorg. Chem.* **1982**, *21*, 2860. (m) Hallam, M. F.; Luke, M. A.; Mingos, D. M. P.; Williams, I. D. *J. Organomet. Chem.* **1987**, *325*, 271. (n) Hunt, C. T.; Matson, G. B.; Balch, A. L. *Inorg. Chem.* **1981**, *20*, 2270. μ-Cp (o) Werner, H.; Kühn, A. *Angew. Chem., Int. Ed. Engl.* **1977**, 412.

10.1021/ic9811392 CCC: \$18.00

Chart 1

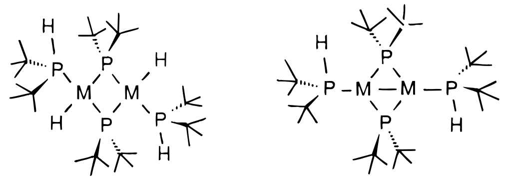

(2) M = Pd
(3) M = Pt

(1) M = Pd
(5) M = Pt

forcing conditions. However it gives the cationic monohydride $[Pt_2(\mu\text{-}PBu^t_2)_2(H)(PBu^t_2H)_2]PF_6$, (**4**)$PF_6$,[14] by oxidant-induced hydride abstraction in the presence of a proton scavenger. We now report that (**4**)PF_6 can be deprotonated to the desired platinum(I) system $[Pt(\mu\text{-}PBu^t_2)(PBu^t_2H)]_2$ (**5**). The carbonylation of the latter complex to $[Pt_2(\mu\text{-}PBu^t_2)_2(PBu^t_2H)(CO)]$ (**6**), whose crystal and molecular structure was determined by X-ray diffraction, the transformation of complex **6** into the CS_2 derivative $[Pt_2(\mu\text{-}PBu^t_2)_2(PBu^t_2H)(\eta^2\text{-}CS_2)]$ (**9**), and the alkylation of complex **5**, yielding $[Pt_2(\mu\text{-}PBu^t_2)_2(PBu^t_2H)(PBu^t_2R)]$ (**12**) (R = *n*-heptyl), are also described.

Results and Discussion

The 30 e^- cation $(\mathbf{4})^+$ [14] (eq 1) can be formally described as being constituted by a tetracoordinated 16 e^- and a tricoordinated 14 e^- platinum(II) centers. Although some degree of metal−metal bonding[14] could partially alleviate the unsaturation of the 14 e^- center, an interesting reactivity could have reasonably been predicted for the complex. Nevertheless the cation is also greatly encumbered, the metal centers are embedded in the envelope of eight *tert*-butyl groups, and, eventually, this feature dominates the chemistry of the species. A symptom of this behavior was given by $(\mathbf{4})^+TCNE^-$, a stable salt that shows no tendency of $TCNE^-$ to saturate the vacancy at the metal, or insert into the Pt−H bond.[14]

In fact, up to now we have found only a single profitable method for the transformation of complex (**4**)PF_6: the reaction with strong bases.

Although (**4**)PF_6 is prepared in the presence of Et_3N and is stable when exposed to an excess of this base, it reacts with stronger bases. For example, by reacting (**4**)PF_6 with an excess of *n*-BuLi (see Experimental Section), we isolated a yellow, highly stable, and unsoluble powder, which has been identified as the platinum(I) derivative $[Pt(\mu\text{-}PBu^t_2)(PBu^t_2H)]_2$ (**5**) (eq 1).

Complex **5**, which does not form by direct reductive elimination of molecular hydrogen from $[Pt(\mu\text{-}PBu^t_2)(H)(PBu^t_2H)]_2$ (**3**), can therefore be achieved by removing the two hydrides of **3** in two separate steps, the first hydride is *formally* removed as H^- [14] and the second as H^+ (eq 1).

We cannot furnish a complete solution characterization of **5** due to its very low solubility in all the common organic solvents (this is a common feature of the *neutral* Pd or Pt bis-phosphido-bridged derivatives **1**, **3**, and **5**).[12,13] Elemental analyses and the IR spectrum of complex **5** (nearly superimposable to the corresponding spectrum of the palladium analogue **1**), as well as all the subsequent results of the reactions given by the complex, agree well with the structure suggested in eq 1, analogous to that of the formerly structurally characterized $[Pt(\mu\text{-}PPh_2)(PPh_3)]_2$.[10a]

Scheme 1

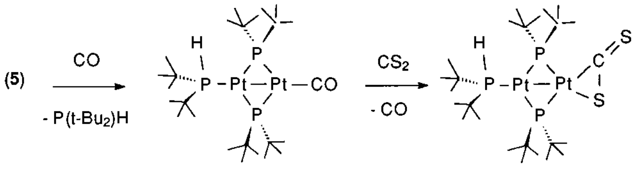

(**6**)

(**9**)

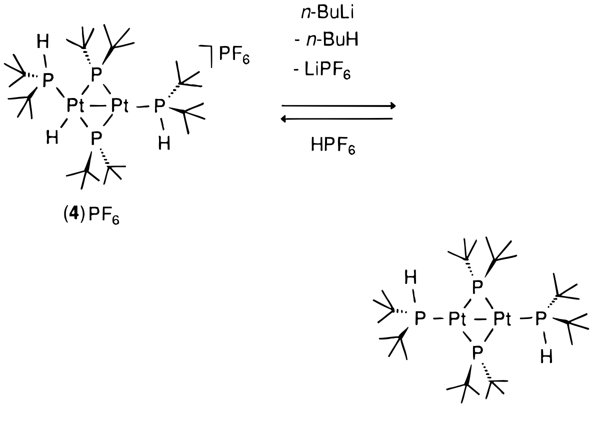

(**4**)PF_6

(**5**)

(1)

To check the reversiblity of the acid−base reaction of eq 1, a toluene suspension of **5** was reacted with HPF_6; the solid rapidly dissolved and the orange solution was shown to contain only (**4**)PF_6 by $^{31}P\{^1H\}$ NMR spectroscopy.[14] The salt was then recovered as an orange microcrystalline solid in high yields.

Carbonylation of 5. Complex **5** was suspended in toluene under 1 Atm of carbon monoxide (Scheme 1). After warming the suspension 4 h at 50 °C, we obtained a yellow solution which contained ($^{31}P\{^1H\}$ NMR) equimolar amounts of $[Pt_2(\mu\text{-}PBu^t_2)_2(PBu^t_2H)(CO)]$, (**6**), and free PBu^t_2H. After workup, complex **6** (Scheme 1) was isolated in good yield and characterized by IR and multinuclear NMR spectroscopy and (see below) by single-crystal X-ray diffraction.

The ^1H NMR spectrum of complex **6** (C_6D_6, 298 K) consists of a doublet of triplets for the P-H proton at 6.22 ppm, with the usual large $^1J_{HP}$ (328 Hz)[11] and a small coupling with the two equivalent μ-P nuclei ($^3J_{HP}$ = 16.5 Hz); ^{195}Pt satellites overlapping the central lines are observable ($^2J_{HPt}$ = 27 Hz). Two distinct signals for the *tert*-butyl protons are found at 1.26 (d, $^3J_{HP}$ = 14.2 Hz, PBu^t_2H) and 1.43 ppm; the latter is a virtual triplet [16] due to the simultaneous couplings of the same order of magnitude with the two bridging P atoms ($^3J_{HP} + {}^5J_{HP}$ = 6.8 Hz, μ-PBu^t_2). The signals are in the expected 1/18/36 integral ratio.

The $^{31}P\{^1H\}$ NMR spectrum (C_6D_6, 298 K), with the atom numbering scheme and the isotopomer's composition, is shown in Figure 1. The spectrum consists of two signals, each given by the sum of the four subspectra due to isotopomers **A**−**D**.

---

(11) (a) Leoni, P.; Pasquali, M.; Sommovigo, M.; Albinati, A.; Pregosin, P. S.; Rüegger, H. *Organometallics* **1996**, *15*, 2047. (b) Leoni, P.; Pasquali, M.; Pieri, G.; Albinati, A.; Pregosin, P. S.; Rüegger, H. *Organometallics* **1995**, *14*, 3143. (c) Sommovigo, M.; Pasquali, M.; Marchetti, F.; Leoni, P.; Beringhelli, T. *Inorg. Chem.* **1994**, *33*, 2651. (d) Leoni, P.; Pasquali, M.; Sommovigo, M.; Laschi, F.; Zanello, P.; Albinati, A.; Lianza, F.; Pregosin, P. S.; Rüegger, H. *Organometallics* **1993**, *12*, 1702.

(12) (a) Leoni, P.; Sommovigo, M.; Pasquali, M.; Sabatino, P.; Braga, D. *J. Organomet. Chem.* **1992**, *423*, 263. (b) Leoni, P. *Organometallics* **1993**, ***12,*** 2432.

(13) Leoni, P.; Manetti, S.; Pasquali, M. *Inorg. Chem.* **1995**, *34*, 749.

(14) Leoni, P.; Pasquali, M.; Fortunelli, A.; Germano, G.; Albinati, A. *J. Am. Chem. Soc.* **1998**, *120*, 9564.

(15) Garrou, P. E. *Chem. Rev.* **1985**, *85*, 171 and references therein.

(16) Crabtree, R. H. *The Organometallic Chemistry of the Transition Metals*, 2nd ed.; J. Wiley & Sons: New York, 1994; Chapter 10, p 237.

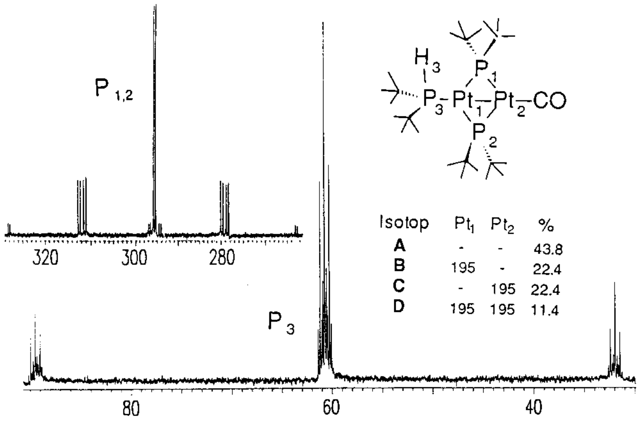

Figure 1. $^{31}P\{^1H\}$ NMR spectrum (C_6D_6, 298 K) of complex **6**, with the numbering scheme and table of isotopomer ratios.

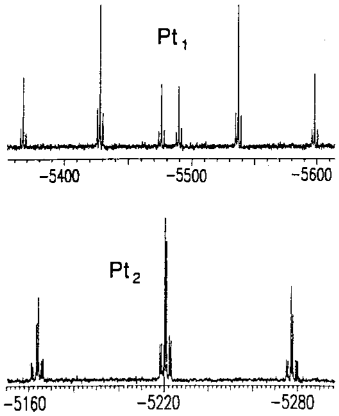

Figure 2. $^{195}Pt\{^1H\}$ NMR spectrum (C_6D_6, 298 K) of complex **6**.

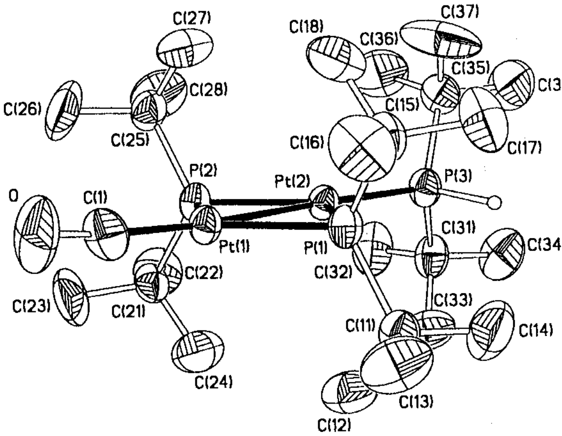

Figure 3. Perspective view of the molecular structure of **6**. Thermal ellipsoids are at 50% probability.

Table 1. NMR Parameters for Complexes **6**, **9**, **10**, and **12**[a]

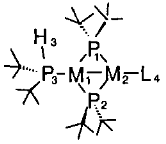	(6) [b]	(9) [c]	(10) [d]	(12) [e]
δ_{P_1}	295.8 d	255.1 dd	268.6 br	272.1 br
δ_{P_2}	295.8 d	302.2 dd	268.6 br	272.1 br
δ_{P_3}	60.7 t	64.9 dd	66.6 dt	60.5 dt
δ_{P_4}	-	-	83.2 br	71.9 dt
δ_{Pt_1}	- 5483 dt	f	f	f
δ_{Pt_2}	- 5220 dt	f	f	f
δ_{H_3}	6.22 dt	5.58	f	6.64
$^2J_{P_1P_2}$	g	250	g	g
$^2J_{P_1P_3}$	38	75	53	42
$^2J_{P_1P_4}$	-	-	h	45
$^2J_{P_2P_3}$	38	9.6	53	42
$^2J_{P_2P_4}$	-	-	h	45
$^3J_{P_3P_4}$	-	-	31	77
$^1J_{P_1Pt_1}$	2623	2207	*ca* 2570	*ca* 2670
$^1J_{P_1Pt_2}$	2431	3175	*ca* 2570	*ca* 2550
$^1J_{P_2Pt_1}$	2623	1106	*ca* 2570	*ca* 2670
$^1J_{P_2Pt_2}$	2431	2987	*ca* 2570	*ca* 2550
$^1J_{P_3Pt_1}$	4660	2866	4964	4570
$^2J_{P_3Pt_2}$	31	97	64	27
$^2J_{P_4Pt_1}$	-	-	h	h
$^1J_{P_4Pt_2}$	-	-	*ca* 2270	4927

[a] δ in ppm, J in Hz. [b] L_4 = CO. [c] $L_4 = \eta^2\text{-}CS_2$. [d] $L_4 = P_{(4)}Bu^t_2Li$. [e] $L_4 = P_{(4)}Bu^t_2$(heptyl). [f] Not measured. [g] Not observed due to chemical and magnetic equivalence. [h] Less than line width.

The former, found at 60.7 ppm and assigned to the secondary phosphine (P_3), consists of a central triplet ($^2J_{P_3P_{1,2}}$ = 38 Hz) for the isotopomer **A**; the isotopomers **B** and **C** give two doublets of triplets with $^1J_{P_3Pt_1}$ = 4660 and $^2J_{P_3Pt_2}$ = 31 Hz, respectively. Isotopomer **D** gives a weak ddt, most of these lines can be observed but do not carry significant additional information. The two equivalent μ-P nuclei resonate at 295.8 ppm, suggesting a short Pt−Pt distance,[15] with a central doublet (isotopomer **A**) flanked by two different dd for isotopomers **B** and **C** ($^1J_{P_{1,2}Pt_1}$ = 2623, $^1J_{P_{1,2}Pt_2}$ = 2431 Hz, assignment facilitated by comparison with the $^{195}Pt\{^1H\}$ NMR spectrum); a weak ddd, due to isotopomer **D**, completes the signal. In the corresponding proton-coupled spectrum, the low field signal is slightly broadened by long-range couplings, while the P_3 signal splits for the large $^1J_{P_3H_3}$ = 328 Hz; a small long-range coupling to the *tert*-butyl protons (13.9 Hz) is also observed.

Two signals are observed in the $^{195}Pt\{^1H\}$ NMR spectrum (C_6D_6, 298 K, Figure 2): Pt_2 gives a triplet of doublets at −5220 ppm (isotopomer **C**, $^1J_{Pt_2P_{1,2}}$ = 2431, $^2J_{Pt_2P_3}$ = 31 Hz) whose lines are flanked by the weak tdd of isotopomer **D** ($^1J_{PtPt}$ = 185 Hz). Pt_1 resonates at −5483 ppm as a triplet of doublets (isotopomer **B**, $^1J_{Pt_1P_{1,2}}$ = 2623, $^1J_{Pt_1P_3}$ = 4660 Hz) with the weak satellites due to isotopomer **D**. Significant absorptions in the IR spectrum (Nujol) were found at 2277 (ν_{PH}) and 1956 (ν_{CO}) cm^{-1}.

Molecular Structure of $[Pt_2(\mu\text{-}PBu^t_2)_2(PBu^t_2H)(CO)]$ (6). Complex **6** crystallizes in the monoclinic space group $P2_1/n$ (No. 14) with 4 molecules in the unit cell. An ORTEP projection of the molecule is shown in Figure 3, and significant bond distances and angles are given in Table 2. The structure has the known main features reported for other $[M(\mu\text{-}PR_2)(L)]_2$ (M = Ni,[17] Pd,[12a,18] Pt[10a]) complexes, with a planar Pt_2P_3C core and two tightly bonded Pt centers which, neglecting the Pt−Pt bond, exhibit a trigonal planar arrangement of the ligands. The Pt(1)−Pt(2) bond distance was found at 2.613(1) Å, close to the Pt−Pt shortest distance (2.774 Å)[19] in platinum metal and within the range of the reported metal−metal bond distances

---

(17) Jones, R. A.; Stuart, A. L.; Atwood, J. L.; Hunter, W. E.; Rogers, R. D. *Organometallics* **1982**, *1*, 1721.

(18) Arif, A. M.; Heaton, D. E.; Jones, R. A.; Nunn, C. M. *Inorg. Chem.* **1987**, *26*, 4228.

(19) Calculated from data reported on card 4-802 of the Powder Diffraction File of JCPDS-ICDD, International Center of Diffraction Data, 1992, 12 Campus Boulevard, Newton Square, PA 19073-3273.

Table 2. Significant Bond Lengths (Å) and Angles (deg) for **6**

Pt(1)−C(1)	1.841(11)	Pt(1)−P(2)	2.311(3)	Pt(1)−P(1)	2.322(3)
Pt(1)−Pt(2)	2.6127(6)	Pt(2)−P(3)	2.256(3)	Pt(2)−P(1)	2.300(3)
Pt(2)−P(2)	2.315(3)	P(1)−C(15)	1.876(11)	P(1)−C(11)	1.908(11)
P(2)−C(21)	1.892(11)	P(2)−C(25)	1.895(11)	P(3)−C(35)	1.878(11)
P(3)−C(31)	1.885(11)	C(1)−O	1.167(13)		

C(1)−Pt(1)−P(2)	118.2(4)	C(1)−Pt(1)−P(1)	130.9(4)
C(1)−Pt(1)−Pt(2)	173.1(4)	P(2)−Pt(1)−P(1)	110.88(9)
P(2)−Pt(1)−Pt(2)	55.69(6)	P(3)−Pt(2)−P(1)	117.18(10)
P(1)−Pt(1)−Pt(2)	55.19(7)	P(3)−Pt(2)−P(2)	131.31(9)
P(1)−Pt(2)−P(2)	111.51(9)	P(3)−Pt(2)−Pt(1)	173.15(7)
P(1)−Pt(2)−Pt(1)	55.98(6)	P(2)−Pt(2)−Pt(1)	55.54(6)
C(15)−P(1)−C(11)	112.6(5)	O−C(1)−Pt(1)	174.5(11)
C(11)−P(1)−Pt(2)	114.8(3)	C(17)−C(15)−P(1)	113.2(8)
C(15)−P(1)−Pt(1)	115.4(4)	C(18)−C(15)−P(1)	104.7(8)
C(11)−P(1)−Pt(1)	118.9(3)	C(14)−C(11)−P(1)	110.7(8)
Pt(2)−P(1)−Pt(1)	68.83(8)	C(27)−C(25)−P(2)	106.1(8)
C(21)−P(2)−C(25)	112.3(5)	C(28)−C(25)−P(2)	113.5(9)
C(21)−P(2)−Pt(1)	112.0(4)	C(26)−C(25)−P(2)	111.0(9)
C(25)−P(2)−Pt(1)	113.7(4)	C(13)−C(11)−P(1)	112.4(8)
C(21)−P(2)−Pt(2)	122.3(4)	C(16)−C(15)−P(1)	112.1(8)
C(25)−P(2)−Pt(2)	119.5(4)	C(23)−C(21)−P(2)	113.3(8)
Pt(1)−P(2)−Pt(2)	68.77(7)	C(24)−C(21)−P(2)	105.0(8)
C(35)−P(3)−C(31)	112.2(5)	C(22)−C(21)−P(2)	112.6(9)
C(35)−P(3)−Pt(2)	116.0(4)	C(34)−C(31)−P(3)	113.5(9)
C(31)−P(3)−Pt(2)	114.8(4)	C(15)−P(1)−Pt(2)	119.8(4)

(Å) in unsupported or ligand-bridged Pt(I) dinuclear derivatives: 2.642(1) in $[Pt_2(\mu\text{-dppm})_2(CO)_2]^{2+}$,[20] 2.6354(8) in the dimetallacylobutenyl $[Pt_2(CO)_2(PPh_3)_2\{C_2(COOMe)_2\}]$,[21] 2.599(1) in $[Pt(CO)(PPh_3)(C_6F_5)]_2$,[22] 2.716(1) in $[Pt_2(\mu\text{-H})(\mu\text{-CO})(dppe)_2]^+$ [23], 2.643(3) in $[Pt_2(\mu\text{-CO})Cl_2(PPh_3)_3]$,[24] 2.636(1) in $[Cp^*Pt(CO)]_2$,[25] and 2.604(1) Å in $[Pt(\mu\text{-PPh}_2)(PPh_3)]_2$.[10a] Other factors suggesting a strong metal−metal interaction are the low-field resonance of the bridging P-nuclei in the $^{31}P\{^1H\}$ NMR spectrum ($\delta_{PH} = 295.8$ ppm) and the sharp Pt−Pμ-Pt angles (68.83(8) and 68.77(7)°).

As generally found in bis-phosphido-bridged derivatives of the group 10 metals, the Pt−P_μ bond distances are longer than the Pt−P_t ones (Pt(2)−P(3) = 2.265(3) and Pt−P_μ(average) = 2.312 Å). Distances pertaining to the carbonyl ligand (Pt(1)−C(1) = 1.841(11) and C(1)−O(1) = 1.167(3) Å) are, respectively, at the lower and higher limits of the corresponding range of distances observed in the rare examples known of Pt(I)-CO-(terminal) derivatives,[20−22,25] which, together with the relatively low value of ν_{CO} (1956 cm^{-1}, compared to 2060−1968 cm^{-1} in refs 20−22 and 25), suggests some degree of back-bonding from the $Pt_2(\mu\text{-PR}_2)_2(PR_3)$ fragment to the carbonyl ligand.

Reaction of 6 with CS$_2$. We have previously shown that the mono-phosphido bridged palladium(I) dinuclear fragments $[Pd_2(\mu\text{-PBu}^t_2)(L)_2]^+$ manifest a good affinity for the carbon disulfide molecule.[11b,26] Both cationic dinuclear and neutral tetranuclear new complexes were prepared, with the CS$_2$ molecule presenting unprecedented coordination modes: a planar $Pd_2(\mu\text{-CS}_2)$ core in $[Pd_2(\mu\text{-PBu}^t_2)(\eta^2{:}\eta^2\text{-CS}_2)(PPh_3)_2]BF_4$, (**7**)BF$_4$,[11b] with a planar tetracoordinate carbon atom, and a butterfly structure in $[Pd_2(\mu\text{-PBu}^t_2)(I)(PPh_3)]_2(CS_2)$ (**8**) with a hexacoordinate carbon atom (Chart 2).[26]

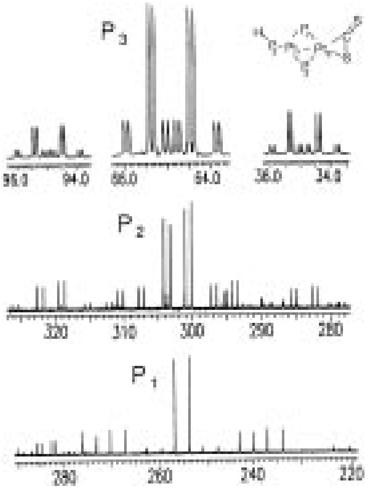

Figure 4. $^{31}P\{^1H\}$ NMR spectrum (C_6D_6, 298 K) of complex **9**.

Chart 2

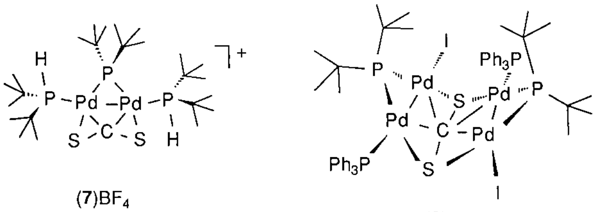

(**7**)BF$_4$

(**8**)

The platinum(I) monocarbonyl **6** reacts at room temperature with an excess of carbon disulfide and is quantitatively transformed into $[Pt_2(\mu\text{-PBu}^t_2)_2(PBu^t_2H)(\eta^2\text{-CS}_2)]$, (**9**, Scheme 1). Due to the unsymmetrical coordination of the CS$_2$ molecule, the $^{31}P\{^1H\}$ NMR (Figure 4) signals of the phosphido ligands lose the equivalence observed in the corresponding spectrum of the carbonyl precursor. Therefore they appear as separate doublets of doublets at 302.2 (P_2) and 255.1 (P_1) ppm. For the same reason the signal assigned to the terminally bonded phosphine (dd at 64.9 ppm) couples with different constants to P_1 and P_2 ($^2J_{P_3P_1} \approx 75$, $^2J_{P_3P_2} \approx 9.6$ Hz). All signals are flanked by the ^{195}Pt satellites that provide the coupling constants reported in Table 1.

The labeled derivative $[Pt_2(\mu\text{-PBu}^t_2)_2(PBu^t_2H)(\eta^2\text{-}^{13}CS_2)]$ (**9***) was prepared analogously, and its $^{31}P\{^1H\}$ NMR spectrum changes as expected: the signal assigned to P_3 appears now as a doublet of triplets due to the coincidence of two out of the three coupling constants ($^3J_{P_3C} = {}^2J_{P_3P_2} = 9$ Hz). The signal assigned to P_1 is only slightly broadened due to the small coupling of this nucleus with the pseudo-cis CS$_2$ carbon, while P_2 appears as a ddd, for the larger value ($^2J_{P_2C} = 46$ Hz) of the coupling with the pseudo-trans CS$_2$ carbon.

Lithiation and Alkylation of 5. In addition to the terminal hydride, complex (**4**)PF$_6$ contains two further potentially acidic protons on the secondary phosphines. As seen above, a 5-fold excess of such a strong base as *n*-BuLi is not sufficient to abstract these protons when **5** is prepared from (**4**)PF$_6$; however, when the reaction was performed with a still higher excess of *n*-BuLi (20:1, or more) a further reaction takes place: only a small amount of **5** precipitated out, while the supernatant solution assumed a deep red color. The solution was analyzed by means of $^{31}P\{^1H\}$ NMR spectroscopy which revealed the presence of $[Pt_2(\mu\text{-PBu}^t_2)_2(PBu^t_2H)(PBu^t_2Li\{Solv\}_x)]$ (**10**, Scheme 2).

---

(20) Fisher, R. J.; Mills, A. J.; Sumner, S.; Brown, M. P.; Thomson, M. A.; Puddephatt, R. J.; Frew, A. A.; Manojlovic-Muir, L.; Muir, K. W. *Organometallics* **1982**, *1*, 1421.

(21) Koie, Y.; Shinoda, S.; Saito, Y.; Fitzgerald, B. J.; Pierpont, C. G. *Inorg. Chem.* **1980**, *19*, 770.

(22) Uson, R.; Fornies, J.; Espinet, P.; Fortuño, C.; Tomás, M.; Welch, A. J. *J. Chem. Soc., Dalton Trans.* **1989**, 1583.

(23) Minghetti, G.; Bandini, A. L.; Banditelli, G.; Bonati, F.; Szostak, R.; Strouse, C.; Knobler, C. B.; Kaesz, H. D. *Inorg. Chem.* **1983**, *22*, 2332.

(24) Bender, R.; Braunstein, P.; Tiripicchio, A.; Tiripicchio-Camellini, M. *J. Chem. Soc., Chem. Commun.* **1984**, 42.

(25) Boag, N. M. *Organometallics* **1988**, *7*, 1446.

(26) Leoni, P.; Pasquali, M.; Fadini, L.; Albinati, A.; Hofmann, P.; Metz, M. *J. Am. Chem. Soc.* **1997**, *119*, 8625.

Scheme 2

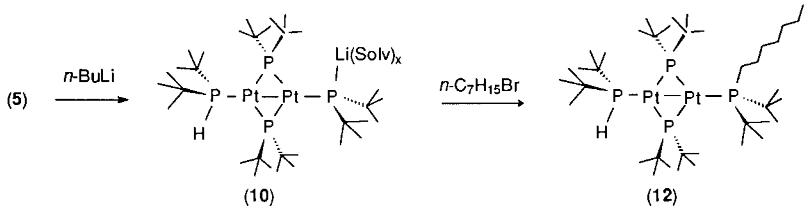

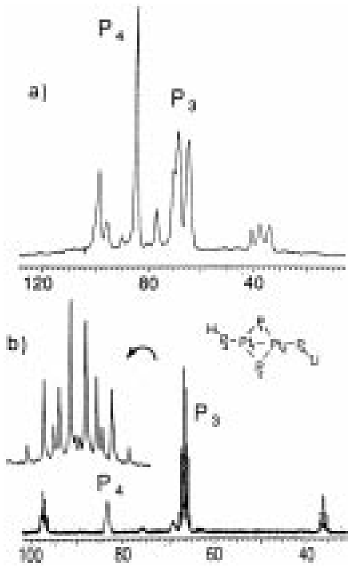

Figure 5. High-field region of the ^{31}P NMR spectrum (toluene, 298 K) of complex **10**; (a) proton coupled, (b) proton decoupled.

Three resonances were in fact observed in the spectrum at 66.6, 83.2, and 268.6 ppm (Figure 5). The first one is well resolved and appears (central multiplet, isotopomer **A**) as a doublet ($^3J_{P_3P_4}$ = 31 Hz) of triplets ($^2J_{P_3P_1} = {}^2J_{P_3P_2}$ = 53 Hz). ^{195}Pt satellites were clearly observable owing to the isotopomers **B** ($^1J_{P_3Pt_1}$ = 4964 Hz), **C** ($^2J_{P_3Pt_2}$ = 64 Hz), and **D**. In the corresponding proton-coupled spectrum the signal split due to a large $^1J_{P_3H}$ (310 Hz) and was therefore assigned to the terminally bonded secondary phosphine P$_3$. The resonances at 83.2 and 268.6 ppm are broadened and considerably weaker than the first in the proton decoupled spectrum; in the proton-coupled spectrum these signals are only slightly broadened and their intensity is comparable to that of the first. Both these evidences indicate clearly the absence of P$-$H bonds on the associated P nuclei, and the resonances are assigned, respectively, to the lithiated nucleus P$_4$ and to the equivalent μ-P nuclei P$_1$ and P$_2$. The line-broadening of these resonances allowed us to evaluate only the largest couplings, which were found at ca. 2270 ($^1J_{P_4Pt_2}$) and ca. 2570 ($^1J_{P_{1,2}Pt_1} \cong {}^1J_{P_{1,2}Pt_2}$). The reasons of this line broadening were not investigated further, although it seems reasonable that species differing in the solvation of the P-bonded lithium are in mutual equilibrium; species where lithium interacts simultaneously with P$_4$ and one of the adjacent bridging nuclei P$_1$ or P$_2$ could also be involved in such equilibria.

As expected, the same reaction was observed when complex **5**, instead of (**4**)PF$_6$, was reacted with a large excess of *n*-BuLi; the reaction was also performed by adding a 1/1 mixture of *n*-BuLi and TMEN, in which case 2 equiv of the base is sufficient to lithiate one of the secondary phosphines. The ^{31}P-{^{1}H} NMR spectrum of the resulting deep red solution was identical to the one described above, except small differences in the chemical shift values. New weak broad resonances were observed at ca. 74 and 255 ppm and were assigned to [Pt(μ-PBu$^t_2$)(PBu$^t_2$Li{Solv}$_x$)]$_2$ (**11**), where both the secondary phosphines have been lithiated.

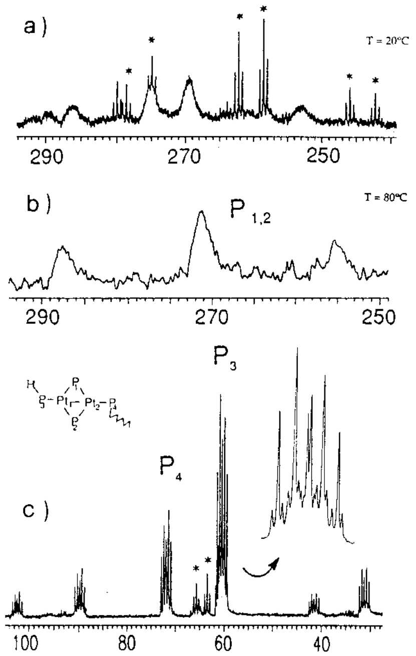

Figure 6. ^{31}P{^{1}H} NMR spectrum (toluene-d_8, 298 K) of complex **12**; low-field region at 293 K (a) and 353 K (b) and high-field region at 293 K (c). Marked peaks have been tentatively assigned to two different rotamers of [Pt(μ-PBu$^t_2$){PBu$^t_2$)(n-heptyl)}]$_2$.

The lithiated derivatives **10** and **11** were not isolated, but the mixture was reacted with an excess of 1-bromoheptane, with the intent to obtain a soluble analogue of complex **5**. Immediately after the addition of the bromoalkane the color of the solution turned orange from deep red, the ^{31}P{^{1}H} NMR spectrum (Figure 6) was analogous to the preceding one, with four groups of resonances assigned to [Pt$_2$(μ-PBu$^t_2$)$_2$(PBu$^t_2$H)-{PBu$^t_2$(n-heptyl)}] (**12**).

The high-field resonances at 60.5 (secondary phosphine, P$_3$) and 71.9 (tertiary phosphine, P$_4$) are well resolved and appear much similar: both of them have a central doublet (mutual coupling, $^3J_{P_3P_4}$ = 77 Hz) of triplets (coupling with the two μ-P nuclei, respectively $^2J_{P_3P_{1,2}}$ = 42 and $^2J_{P_4P_{1,2}}$ = 45 Hz) flanked by ^{195}Pt satellites due to a large coupling with the adjacent metal ($^1J_{P_3Pt_1}$ = 4750 and $^1J_{P_4Pt_2}$ = 4927 Hz, respectively) and a small coupling to the distant one (respectively $^2J_{P_3Pt_2}$ = 27 Hz and $^2J_{P_4Pt_1}$ less than line width (3 Hz)). Significant differences are the following: the signal at 71.9 ppm is weaker and is only slightly broadened in the corresponding proton-coupled spectrum, while the greater resonance at 60.5 ppm split in a broad doublet ($^1J_{PH}$ = 310 Hz).

The bridging phosphides P$_1$ and P$_2$ are unequivalent at room temperature, and give broad resonances at 269.3 and 274.9 ppm; only the larger $^1J_{PPt}$ couplings (ca. 2670 and 2550 Hz, respectively) can be appreciated because of line-broadening (half-height width 200 Hz). The two signals coalesce at 70 °C in a single broad resonance centered at 272.1 ppm. The nonequivalence of P_1 and P_2 at room temperature should probably be assigned to a slow rotation of the tertiary phosphine around the Pt_2-P_4 bond. The complex is in fact severely crowded for the presence of eight *tert*-butyl substituents. Steric crowding is probably also the main obstacle to the direct substitution of the secondary phosphines contained in **5**; the latter remains in fact unchanged after 10 days in the presence of a large excess of trimethylphosphine.

Conclusions

A convenient access to the bis-phosphido-bridged platinum(I) dinuclear derivative $[Pt(\mu\text{-}PBu^t_2)(PBu^t_2H)]_2$ (**5**) has been presented. Both **5** and its platinum(II) conjugate acid $[Pt_2(\mu\text{-}PBu^t_2)_2(H)(PBu^t_2H)_2]PF_6$, (**4**)$PF_6$, proved much less reactive than expected, being inert to even the substitution of the PBu^t_2H molecules with phosphines with a small cone angle as PMe_3. The low reactivity is probably due to a high steric congestion around the metal centers wrapped by the eight *tert*-butyl substituents on the phosphorus atoms. This is also suggested by the behavior of complex **12** (related to **5** by the substitution of a PBu^t_2H with a PBu^t_2(*n*-heptyl) molecule), where a slight increase of the cone angle of one of the phosphines imposes a significant kinetic barrier to even the rotation around the $Pt-PR_3$ bond. Nevertheless, a suitable method for the transformation of **5** was found, as its reaction with CO affords the monocarbonyl $[Pt_2(\mu\text{-}PBu^t_2)_2(PBu^t_2H)(CO)]$ (**6**). This is one of the rare examples of platinum(I) terminally bonded carbonyls and is much less encumbered than is precursor **5**. On its own, **6** is the precursor of the CS_2 complex $[Pt_2(\mu\text{-}PBu^t_2)_2(PBu^t_2H)(\eta^2\text{-}CS_2)]$ (**9**), which could have been, but is not, formed by the reaction of **5** with carbon disulfide.

The structure of complex **6** deserves a final comment. We have recently shown that monophosphido-bridged dipalladium(I) fragments exhibit cooperation of the metal centers when binding carbon disulfide,[11b] as well as other polyunsaturated molecules;[11a] on the contrary, the CS_2 molecule is η^2 coordinated to a single platinum center in complex **9**, with the rest of the molecule formally behaving as a single PtP_2 tridentate large ligand to the same metal center. This type of behavior could be interesting in itself, but it seems clear that if one wants the two metal centers to concur in the coordination and, possibly, the activation of small polyfunctional molecules, one of the phosphido ligands must be removed. A possible approach to this target will be reported in future articles.

Experimental Section

General Data. All reactions were carried out under a nitrogen atmosphere, by using standard Schlenk techniques. $[Pt_2(\mu\text{-}PBu^t_2)_2(H)(PBu^t_2H)_2]PF_6$ was prepared as previously described.[14]

Solvents were dried by conventional methods and distilled under nitrogen prior to use. IR spectra (Nujol mulls, KBr) were recorded on a Perkin-Elmer FT-IR 1725X spectrophotometer. NMR spectra were recorded on a Varian Gemini 200 BB instrument; frequencies are referenced to Me_4Si (^1H), 85% H_3PO_4 (^{31}P), and H_2PtCl_6 (^{195}Pt).

Preparation of $[Pt(\mu\text{-}PBu^t_2)(PBu^t_2H)]_2$ (5). A 1.6 M *n*-hexane solution of *n*-BuLi (0.625 mL, 1.0 mmol) was dropped into a THF (20 mL) solution of $[Pt_2(\mu\text{-}PBu^t_2)_2(H)(PBu^t_2H)_2]PF_6$ [(**4**)PF_6, 223 mg, 0.195 mmol]. After 15 min the yellow color of the solution had discharged and the pale yellow solid which precipitated out was filtered, washed with *n*-hexane, and vacuum-dried, yielding 121 mg (64%) of **5**. Anal. Calcd for $C_{32}H_{74}P_4Pt_2$: C, 39.5; H, 7.67. Found: C, 38.8; H, 7.52. IR (Nujol, KBr): 2259 (s) (ν_{PH}) cm^{-1}. Being nearly insoluble in all the common organic solvents the solid was used for the following reaction without further purification.

Table 3. Crystal Data and Structure Refinement for **6**

empirical formula $C_{25}H_{55}OP_3Pt_2$	fw 854.78
$a = 9.0910(12)$ Å	space group $P2_1/n$ (No. 14)
$b = 30.527(4)$ Å	$T = 293(2)$ K
$c = 11.903(2)$ Å	$\lambda = 0.71073$ Å
$\beta = 93.78(2)$ deg	$\rho_{obs} = 1.722$ g cm^{-3}
$V = 3296.1(8)$ Å^3	$\mu = 86.38$ cm^{-1}
$Z = 4$	$R(F_o) = 0.0378^a$
	$Rw(F_o^2) = 0.0826$

[a] $R(F_o) = \sum||F_o| - |F_c||/\sum|F_o|$; $Rw(F_o^2) = [\sum[w(F_o^2F_c^2)^2]/\sum[w(F_o^2)^2]]^{1/2}$; $w = 1/[\sigma^2(F_o^2) + (0.0243P)^2 + 0.57Q]$ where $P = [\mathrm{Max}(F_o^2,0) + 2F_c^2]/3$.

Preparation of $[Pt_2(\mu\text{-}PBu^t_2)_2(PBu^t_2H)(CO)]$ (6). Complex **5** (214 mg, 0.22 mmol) was suspended in toluene (20 mL). The colorless suspension was stirred 1h at 60 °C under 1 atm of carbon monoxide: the solid disappeared slowly leaving an orange-red clear solution. Most of the solvent was evaporated, the residue was dissolved in MeCN (10 mL) and complex **6**, which precipitated out slowly as a red crystalline solid, was filtered, washed with MeCN, and vacuum-dried (130 mg, 0.152 mmol, 69%). Anal. Calcd for $C_{25}H_{55}OP_3Pt_2$: C, 35.1; H, 6.49. Found: C, 34.8; H, 6.62. IR (Nujol, KBr): 2277 (m) (ν_{PH}), 1956 (s) (ν_{CO}) cm^{-1}. See Table 1 for ^1H, ^{31}P, and ^{195}Pt NMR spectra.

Preparation of $[Pt_2(\mu\text{-}PBu^t_2)_2(PBu^t_2H)(\eta^2\text{-}CS_2)]$ (9). Carbon disulfide (2 mL, 33 mmol) was added to a DME (5 mL) solution of complex **6** (240 mg, 0.28 mmol). After 12 h at room temperature the orange solution turned deep-red. The solution was concentrated to ca. 2 mL, and acetone (10 mL) was added. A deep red solid precipitated out and was filtered, washed with acetone, and vacuum-dried (175 mg, 69%). Anal. Calcd for $C_{25}H_{55}P_3Pt_2S_2$: C, 33.3; H, 6.14. Found: C, 33.2; H, 6.09. IR (Nujol, KBr): 2258 (ν_{PH}) cm^{-1}. ^1H NMR (C_6D_6, 293 K) δ (ppm) 5.58 (ddd, $^1J_{PH} = 339$ Hz, $^3J_{PH} = 12$, 21 Hz, P-*H*), 1.47 (d, $^3J_{PH} = 16$ Hz, C*H*$_3$), 1.39 (d, $^3J_{PH} = 15$ Hz, C*H*$_3$), 1.16 (d, $^3J_{PH} = 15$ Hz, C*H*$_3$). See Table 1 for ^{31}P NMR parameters.

Preparation of $[Pt_2(\mu\text{-}PBu^t_2)_2(PBu^t_2H)\{PBu^t_2(n\text{-heptyl})\}]$ (12). A 1.6 M *n*-hexane solution of *n*-BuLi (1.92 mL, 3.07 mmol) and tetramethylethylenediamine (0.47 mL, 3.11 mmol) were added to a toluene (20 mL) suspension of complex **5** (150 mg, 0.154 mmol). After being stirred at room temperature for 12 h the yellow solid disappeared completely, leaving a deep red solution, which was shown ($^{31}P\{^1H\}$ NMR, see results and discussion) to contain the monolithiated $[Pt_2(\mu\text{-}PBu^t_2)_2(PBu^t_2H)\{PBu^t_2Li(solv)_x\}]$. The color of the solution turned quickly yellow after the addition of *n*-bromoheptane (0.48 mL, 3.07 mmol). The solution was stirred for 1 h at room temperature and concentrated to ca. 2 mL, and complex **12** was precipitated by adding acetone (15 mL) and then filtered and vacuum-dried (120 mg, 0.112 mmol, 73%). Anal. Calcd for $C_{39}H_{88}P_4Pt_2$: C, 43.7; H, 8.28. Found: C, 43.2; H, 8.19. IR (Nujol, KBr): 2250 (ν_{PH}) cm^{-1}. NMR data in Table 1.

Crystal Structure Determination. A red prismatic crystal of $[Pt_2(\mu\text{-}PBu^t_2)_2(PBu^t_2H)(CO)]$ obtained from a MeCN solution was glued at the end of a glass fiber and was mounted on a Siemens P4 automatic single-crystal X-ray diffractometer equipped with graphite monochromatized Mo Kα radiation, obtaining the crystal parameters listed in Table 3. A redundant set of intensities was collected by testing the crystal stability and alignment with three standard reflections measured every 97 measurements. The collected intensities were corrected for Lorentz and polarization effects and for absorption by using a Gaussian method based on the crystal shape and size.[27] The internal reliability factor $R(\mathrm{int}) = \sum|F_o^2 - F_o^2(\mathrm{mean})|/\sum|F_o^2|$ after the corrections, calculated on the equivalent reflections, was obtained refining 299 parameters on 4746 intensity data with $I > 2\sigma(I)$ and is shown in Table 3. The space group was univocally established on the basis of systematic extinctions and the structure was solved by using the automatic Patterson method contained in the SHELXTL[27] program. All the heavy atoms were located in the next Fourier map. The hydrogen atoms were in part located on the difference Fourier map and in part placed in calculated positions. The final refinement cycle was performed by using

---

(27) Sheldrick, G. M. *SHELXTL*, Release 5.03; Siemens Analytical X-ray Instruments Inc.: Madison, WI, 1992.

anisotropic thermal factors for the heavy atoms and imposing to hydrogen atoms coordinates to "ride" on the heavy atoms they were connected. The reliability factors of the refinement, listed at the bottom of Table 3, were obtained by using 299 parameters and 4746 intensity data with $I > 2\sigma(I)$.

Acknowledgment. CNR (Rome) and Ministero dell'Università e della Ricerca Scientifica e Tecnologica (MURST) are gratefully acknowledged for financial support.

Supporting Information Available: An X-ray crystallographic file, in CIF format, for the structure determination of **6** is available free of charge via the Internet at http://pubs.acs.org.

IC9811392